

Two-Color Far-Field Fluorescence Nanoscopy

Gerald Donnert,* Jan Keller,* Christian A. Wurm,* Silvio O. Rizzoli,[†] Volker Westphal,* Andreas Schönle,* Reinhard Jahn,[†] Stefan Jakobs,* Christian Eggeling,* and Stefan W. Hell*

Max Planck Institute for Biophysical Chemistry, Departments of *NanoBiophotonics and [†]Neurobiology, 37070 Göttingen, Germany

ABSTRACT We demonstrate two-color fluorescence microscopy with nanoscale spatial resolution by applying stimulated emission depletion on fluorophores differing in their absorption and emission spectra. Green- and red-emitting fluorophores are selectively excited and quenched using dedicated beam pairs. The stimulated emission depletion beams deliver a lateral resolution of <30 nm and 65 nm for the green and the red color channel, respectively. The ~5 nm alignment accuracy of the two images establishes the precision with which differently labeled proteins are correlated in space. Colocalized nanoscopy is demonstrated with endosomal protein patterns and by resolving nanoclusters of a mitochondrial outer membrane protein, Tom20, in relation with the F₁F₀ATP synthase. The joint improvement of resolution and colocalization demonstrates the emerging potential of far-field fluorescence nanoscopy to study the spatial organization of macromolecules in cells.

Received for publication 21 January 2007 and in final form 6 February 2007.

Address reprint requests and inquiries to Stefan W. Hell, E-mail: hell@4pi.de.

The commonly used variants of lens-based (far-field) fluorescence microscopy would be ideal for exploring the distribution of proteins in cells if their spatial resolution were not limited by diffraction to about a half of the wavelength of light: $\lambda/2 \sim 200$ nm (1). Stimulated emission depletion (STED) microscopy (2) is an emerging microscopy technique that, although still using regular lenses, fundamentally overcomes the diffraction barrier. In its single-point scanning variant, STED microscopy uses two coaligned beams: one for excitation, and a second one, with a longer wavelength, to de-excite the fluorophore by stimulated emission. Whereas the excitation beam is regularly focused, the STED beam forms a doughnut in the focal plane, featuring a zero at the center. Superposing the first with the latter confines fluorescence emission toward the center, thus narrowing the spot from which fluorescence may originate. The breaking of the diffraction barrier is based on the fact that the excited state population decreases almost exponentially with the intensity I of the STED beam. Increasing I confines the fluorescent spot continually. If we define I_s as the intensity at which the probability of fluorescence is reduced to $1/e$, the lateral resolution is approximated by $\Delta r = \lambda / (2n \sin \alpha \sqrt{1 + I/I_s})$, with $n \sin \alpha = NA$ denoting the numerical aperture of the lens (3). Ideally, the spatial resolution can be improved to the molecular scale.

So far, STED microscopy has exhibited a resolution of <20 nm (4,5). Moreover, it has been key to answering several biology questions (6). However, in all these studies, STED was implemented with a single color only, meaning that just a single molecular species could be mapped out in the cell. Investigating the spatial relationship of two or more biomolecules at the nanoscale has been impossible, because this task requires at least two color channels. Although molecular proximities <10 nm can be detected through Förster Resonance Energy Transfer using standard fluores-

cence microscopes (7), the nanoscale organization of the (colocalizing) proteins remained elusive.

Here, we demonstrate the viability of STED microscopy with two different fluorophores, particularly with green and red fluorescence emission. The excitation of the green emitters is performed at 470 nm using a laser diode providing 100 ps pulses. STED of these dyes is performed by an optic parametric amplifier providing 300 ps pulses at a wavelength of 603 nm. The red dyes are excited at 635 nm with a similar diode, whereas the corresponding STED pulses are extracted from a regenerative Ti:sapphire amplifier operating at 780 nm. In fact, our system is an extension of the one detailed in Donnert et al. (5) (Supplementary Material). A time difference of 4 μ s between successive pulse pairs ensures that molecules that are occasionally trapped in a dark state with a lifetime <4 μ s can relax in the interim. Dubbed T- or D-Rex, this illumination modality reduces photobleaching mediated by transient dark states, thus allowing for greater I/I_s (5). Since the excitation pulses were triggered by the basic frequency of the amplifier (250 kHz), the synchronization of the pulses did not pose additional challenges in realizing two-color STED. Attention required the fact that the STED beam for the short-wavelength dye may excite its long-wavelength complement. This issue has been solved by recording the red emitter first.

Fig. 1 displays the measured excitation and doughnut spots in the focal plane (transverse point-spread function, PSF) of the oil immersion lens used (Planapo 100 \times , Leica Microsystems, Wetzlar, Germany). The nanoresolution of the system was first verified using green and red fluorescent beads (known as “yellow-green” and “crimson” fluorescent beads from Molecular Probes, Eugene, OR) of 24 ± 4 nm

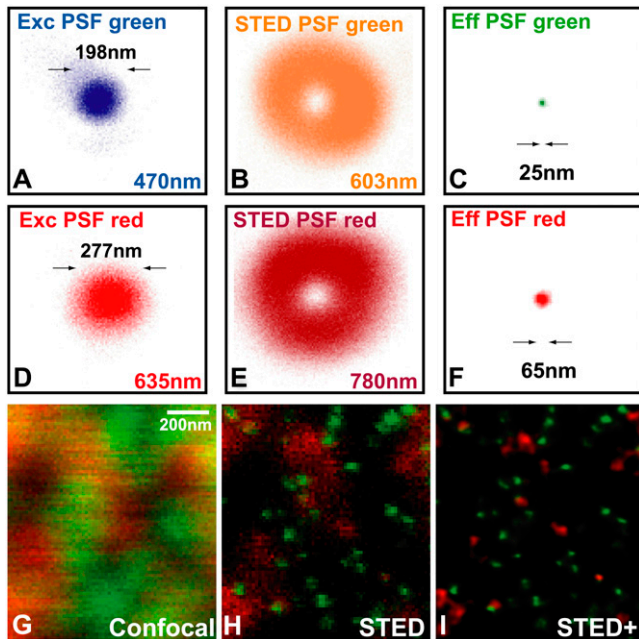


FIGURE 1 Two-color STED microscopy. Excitation and STED PSFs for the green (A and B) and the red (D and E) fluorescence channel. C and F give an upper bound for the effective PSF of the STED microscope under the conditions applied; note the 7.9 \times and 4.3 \times reduction in full-width at half-maximum as compared to the excitation spot. Randomly dispersed green and red fluorescent beads exemplify the resolution gain: confocal (G), STED plain data (H), and STED plus a Richardson-Lucy deconvolution (I). Deconvolution slightly further improved the resolution.

specified diameter, with emission at 500–530 nm and 640–670 nm, respectively. In the absence of STED, the resolution is that of a confocal microscope. Applying intensities $I_{\text{STED}(600\text{nm})}^{\text{max}} = 3.4 \text{ GW/cm}^2$ and $I_{\text{STED}(780\text{nm})}^{\text{max}} = 1.1 \text{ GW/cm}^2$ at the doughnut crest reduced the extent of the fluorescence spot. Probing the spot with 35 yellow-green and 30 crimson beads, gave a full-width at half-maximum of $25 \pm 5 \text{ nm}$ and $65 \pm 11 \text{ nm}$, respectively (Fig. 1, C and F, and Supplementary Material). Since the finite bead size is still contained in these values, they represent an upper bound for the resolution under these conditions (5). The comparatively poorer resolution in the red channel is due to the fact that, in our laser system, the λ of the red STED beam (780 nm) was not tunable and hence not fully adaptable to the fluorophores in use. Even so, the resolution in the red channel is 4.3 \times beyond the diffraction barrier.

Fig. 1, G and H, compares a two-color confocal image of a bead mixture on a coverslip with its STED counterpart. Correct overlay of the corresponding images was ensured as outlined in the Supplementary Material. The pixel dwell time was 3 and 5 ms for the green and the red channel, respectively; the pixel size was $15 \times 15 \text{ nm}$ throughout. The focal peak intensities of the excitation pulses were $I_{470\text{nm}} = 4.2 \text{ MW/cm}^2$ and $I_{635\text{nm}} = 4.9 \text{ MW/cm}^2$. Whereas the confocal image features extended blobs, the STED image

separates the majority of the beads (Fig. 1 H). In Fig. 1 I, we also applied a Richardson-Lucy deconvolution (Supplementary Material) on the STED data using the measured PSF of the STED microscope as extracted from Fig. 1, C and F.

Next we performed immunofluorescence nanoscopy using the organic fluorophore Atto532 for the green (530–570 nm) and Atto647N for the red channel (660–700 nm). In the first experiment, we prepared a fraction of pheochromocytoma (PC12) cells, which is a neuroendocrine cell line, enriched in early endosomes. Fig. 2 displays two synaptic vesicle proteins in endosomes: synaptophysin (green) and synaptotagmin I (red). STED was performed with $I_{\text{STED}(600\text{nm})}^{\text{max}} = 1.2 \text{ GW/cm}^2$ and $I_{\text{STED}(780\text{nm})}^{\text{max}} = 0.7 \text{ GW/cm}^2$. To maximize their information content, both the confocal and the STED data were subject to a linear deconvolution (Supplementary Material). Correct overlay of both channels was ensured by double-stained (“yellow-green plus crimson”) fluorescence beads that we added to the sample (arrows, Fig. 2 D). These beads allowed us to overlay both color channels with an accuracy of $\pm 5 \text{ nm}$ (Supplementary Material). Whereas the more abundant protein, synaptophysin, forms ring-shaped domains, synaptotagmin I exhibits point-like distributions that largely colocalize with the synaptophysin-containing structures (Fig. 2, B and D). Fig. 2 E displays a line profile through synaptotagmin I and synaptophysin agglomerations with the corresponding centers of gravity being $25 \pm 5 \text{ nm}$ apart. We surprisingly found that not all synaptic vesicle proteins occupy the same sites on the endosomes.

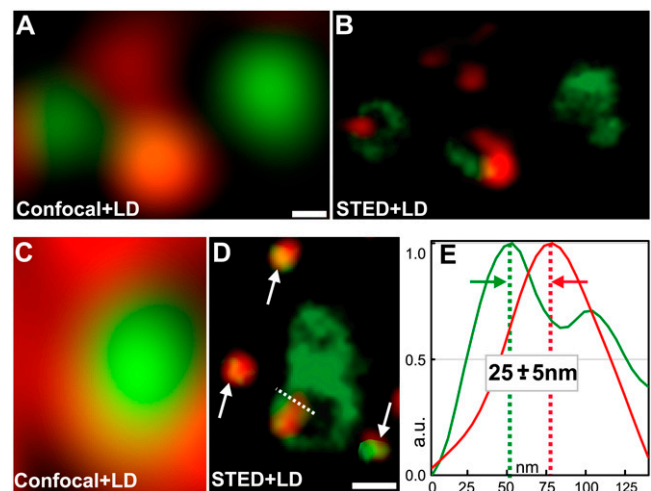


FIGURE 2 Synaptic proteins synaptotagmin I (red) and synaptophysin (green) on endosomes. (A and C) Confocal references and (B and D) STED images (both linearly deconvolved) revealing ring-shaped synaptophysin domains, whereas synaptotagmin I mainly forms dotted structures. We added double-labeled fluorescence beads to the sample, which were not resolved in the confocal image but in the corresponding STED image (arrows in D, green look-up table adjusted for the beads relative to the rest of the image). Dual-color beads allowed for a colocalization precision of $\sim 5 \text{ nm}$. (E) Colocalization profiles of proteins (along white dotted line in D). Scale bar, 100 nm.

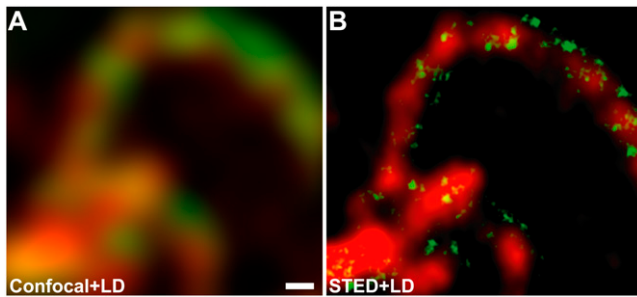


FIGURE 3 Mitochondria labeled with antibodies specific for the F_1F_0 ATP synthase (red) and the TOM complex (green). Unlike the confocal (A), the STED image (B) reveals nanoscale protein distribution patterns; in both images the raw data were further enhanced by a linear deconvolution (LD). The TOM complex is located in distinct clusters (at the mitochondrial surface, green pattern in B). The visualization of the distribution of the F_1F_0 ATP shows a homogeneous staining pattern (red in B). Scale bar, 200 nm.

Finally, we imaged two mitochondrial proteins, namely the α -subunit of the F_1F_0 ATP synthase complex and Tom20 in mammalian (PtK2) cells with $I_{\text{STED}(600\text{nm})}^{\text{max}} = 0.9 \text{ GW/cm}^2$ and $I_{\text{STED}(780\text{nm})}^{\text{max}} = 0.7 \text{ GW/cm}^2$. Electron microscopy reportedly revealed that the F_1F_0 ATP synthase complex is densely packed within the mitochondrial inner membrane (8). Tom20 is a component of the translocase of the outer mitochondrial membrane. Mediating the transport of nuclear encoded mitochondrial preproteins across the outer membrane, the TOM complex has been suggested to be enriched where the inner and the outer membranes are in close proximity. Nonetheless, its spatial distribution remained largely elusive. This partly stems from the challenges of applying immunolabeling in electron microscopy and from the inability of standard fluorescence microscopy to resolve on the nanoscale.

Although the two-color STED recordings confirm the nearly homogeneous distribution of the F_1F_0 ATP synthase (Fig. 3), they reveal for the first time that Tom20 is localized in nanosized clusters. We have reinforced this finding by reverting the labeling: the TOM complex was tagged with the red-labeled antibody whereas the F_1F_0 ATP synthase with the green one (Fig. 4). Again, the TOM complex appeared in nanosized clusters. We expect the two-color nanoresolution of STED microscopy to help elucidate the TOM20 cluster formation and the correlation of these clusters with other mitochondrial morphologies.

A number of technical improvements are foreseeable already. Implementing a tunable STED beam for the red color will bring the red channel resolution up to the 20–30 nm values that are now attained with the green channel. Recent advancements in photonic crystal fiber technology and of laser physics should greatly simplify dual or even three-color implementations of STED microscopy. Adding a diffraction-limited third channel is readily possible.

In conclusion, we have demonstrated the viability of dual-color fluorescence nanoscopy. The progress in biological microscopy reported herein should facilitate the imaging of

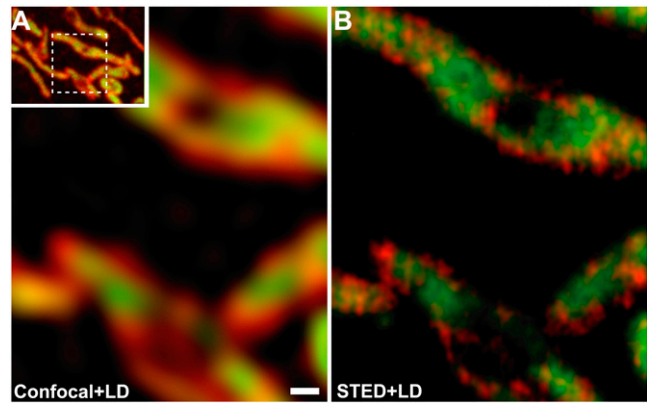


FIGURE 4 Mitochondria with labeled F_1F_0 ATP synthase (green) and TOM complex (red); reverted antibody labeling as compared to Fig. 3. Again, the TOM complex appears as clusters; unlike the confocal (left), the STED recording (right) resolves the TOM complex clusters. In both recordings, the raw data were subject to a linear deconvolution (LD) with the respective PSF. (Inset) Low magnification image. Scale bar, 200 nm.

protein colocalizations in cells with hitherto unprecedented detail. STED microscopy should be a powerful technique to image colocalized protein distributions, because it retains most of the advantages of confocal microscopy, including the ability to image organelles in intact cells.

SUPPLEMENTARY MATERIAL

An online supplement to this article can be found by visiting BJ Online at <http://www.biophysj.org>.

ACKNOWLEDGMENTS

We thank A. Engler and B. Harke for technical assistance.

REFERENCES and FOOTNOTES

1. Abbe, E. 1873. Beiträge zur Theorie des Mikroskops und der mikroskopischen Wahrnehmung. *Arch. f. Mikr. Anat.* 9:413–420.
2. Hell, S. W., and J. Wichmann. 1994. Breaking the diffraction resolution limit by stimulated emission: stimulated emission depletion microscopy. *Opt. Lett.* 19:780–782.
3. Hell, S. W. 2003. Toward fluorescence nanoscopy. *Nat. Biotechnol.* 21:1347–1355.
4. Westphal, V., and S. W. Hell. 2005. Nanoscale resolution in the focal plane of an optical microscope. *Phys. Rev. Lett.* 94:143903.
5. Donnert, G., J. Keller, R. Medda, M. A. Andrei, S. O. Rizzoli, R. Lühmann, R. Jahn, C. Eggeling, and S. W. Hell. 2006. Macromolecular-scale resolution in biological fluorescence microscopy. *Proc. Natl. Acad. Sci. USA.* 103:11440–11445.
6. Willig, K. I., S. O. Rizzoli, V. Westphal, R. Jahn, and S. W. Hell. 2006. STED-microscopy reveals that synaptotagmin remains clustered after synaptic vesicle exocytosis. *Nature.* 440:935–939.
7. Jares-Erijman, E. A., and T. M. Jovin. 2003. FRET imaging. *Nat. Biotechnol.* 21:1387–1395.
8. Allen, R. D., C. C. Schroeder, and A. K. Fok. 1989. An investigation of mitochondrial inner membranes by rapid-freeze deep-etch techniques. *J. Cell Biol.* 108:2233–2240.